J Fluoresc (2013) 23:865–875
DOI 10.1007/s10895-013-1229-3

SHORT COMMUNICATION

The Effects of Different Solvents and Excitation Wavelength on the Photophysical Properties of Two Novel Ir(III) Complexes Based on Phenylcinnoline Ligand

Jing Xu · Chaolong Yang · Bihai Tong · Yunfei Zhang · Liyan Liang · Mangeng Lu

Received: 23 January 2013 / Accepted: 30 April 2013 / Published online: 9 May 2013

Abstract Two novel cyclometalated iridium(III) complexes, $Ir(pcl)_2(pic)$ and $Ir(pcl)_2(fpic)$ (pcl: 3-phenylcinnoline, pic: picolinic acid, fpic: 5-fluoro-2-picolinic acid) were synthesized and characterized by FTIR, ^1H NMR spectroscopy, UV-vis, PL, and MALDI-TOF. These two Ir-complexes geometry were predicted using the Sparkle/PM6 model and suggested to a chemical environment of very low symmetry around the Ir ions (C_1). The PL spectrum of $Ir(pcl)_2(pic)$ and $Ir(pcl)_2(fpic)$ indicated that these complex belonged to red light emission, and maximum emission wavelength located at 647 and 641 nm, respectively. Most importantly, the effects of different solvents on their photoluminescent properties were detailed investigated. The results indicated that the polarity of solvent played an important role for their emission spectra. With introducing fluoro group to the pyridyl ring, the maximum emission wavelength of $Ir(pcl)_2(fpic)$ was blue shifted about 6 nm, and the quantum yield was slightly higher than that of $Ir(pcl)_2(pic)$. In addition, the thermal properties of these two Ir-complexes were measured by TGA, and results indicated that they had relative good thermal properties.

Keywords Iridium(III) complex · Phosphorescence · Photoluminescence · Photophysical properties

Introduction

Cyclometalated iridium(III) complexes have been recently shown to be excellent candidates for use in light-emitting electrochemical cells (LECs) [1–3], oxygen sensing [4–7], bioanalytical applications [8–10] and organic light-emitting diodes (OLEDs) [11, 12], because of their high phosphorescence efficiency and relatively short excited state lifetime [13]. As the phosphorescent materials, both singlet and triplet excitons can be harvested for light emission [14]. For cyclometalated iridium(III) complexes, the strong spin-orbit coupling induced by the central metal ion leads to mixing of the singlet and triplet excited states, consequently changing the spin-forbidden nature of triplet transition to spin-allowed. So far, though many iridium complexes with RGB (red, green, blue) emissions have been developed, efficient red-emitting materials are still scarce [15]. Moreover, it is previously found that the emission color of iridium(III) complexes can be strongly governed by the cyclometalating ligands in comparison to the ancillary ligands [16]. But this standpoint has been changed, since the emission colors of $Ir(dfppy)_2(LX)$ complexes can be tuned from blue to red by modulating the ancillary ligand [17]. The results demonstrated that the substitution of ancillary ligand could change the energy level of highest occupied molecular orbital (HOMO) or lowest

Electronic supplementary material The online version of this article (doi:10.1007/s10895-013-1229-3) contains supplementary material, which is available to authorized users.

J. Xu · C. Yang · B. Tong · Y. Zhang · L. Liang · M. Lu (✉)
Guangzhou Institute of Chemistry, Chinese Academy of Sciences, Guangzhou 510650, People's Republic of China
e-mail: mglu@gic.ac.cn

J. Xu · C. Yang · Y. Zhang
University of Chinese Academy of Sciences, Beijing 100039, People's Republic of China

B. Tong
College of Metallurgy and Resources, Anhui University of Technology, Ma'anshan, Anhui 243002, People's Republic of China

unoccupied molecular orbital (LUMO). Therefore, using appropriate ancillary ligands provide potential strategies for phosphorescence color tuning as well as cyclometalating ligands [18].

In the previous work, cyclometalated iridium(III) complexes with phenylphthalazine derivatives have been proven to be promising red emitters in OLEDs [19–21]. Tong et al. reported one red-light materials with $Ir(MPCPPZ)_3$ as a dopant [19]. Fang et al. also obtained a novel ligand with excellent performance by introducing carbazole unit into a phenylphthalazine derivative [20]. Using quantum chemistry calculations, Mi et al. demonstrated that the ligands which have the structure of an sp^2-hybid N-atom adjacent to the chelating N-atom (represented as CˆN=N) are superior to these analogues with chelating N-atoms adjacent to sp^2 C-atoms (represented as CˆN=CH) due to the shorter bonding length and the stronger bonding strength between the chelating N-atom and Ir-atom [21]. Phenylcinnoline derivatives, having the resemblance of CˆN=N structure, are expected to obtain good performances by coordinating with iridium(III). Until now, there are limited reports about phenylcinnoline derivatives utilized as the cyclometalated ligand in iridium(III) complex.

In this work, we report two novel, red emissive phosphorescent Ir(III) complexes $Ir(pcl)_2(pic)$ and $Ir(pcl)_2(fpic)$, composed of 3-phenylcinnoline serving as cyclometalating ligand. Moreover, picolinic acid and 5-fluoro-2-picolinic acid have been utilized as ancillary ligand in order to investigate the differences between $Ir(pcl)_2(pic)$ and $Ir(pcl)_2(fpic)$ by introducing fluoro group in the pyridyl ring. The synthesis, photophysical, thermal and electrochemical properties of these complexes are studied, and the influences of solvent and excitation wavelength are also detailed discussed.

Materials and Methods

Materials and Characterization

The solvents were purified by routine procedures and distilled under an atmosphere of dry nitrogen before use. All reagents used were of analytical grade, and were purchased from Aldrich. FT-IR spectra were carried out using a Tensor 27 (Bruker) Fourier Transform Infrared Spectrometer. NMR spectra were taken on a DRX-400 MHz (Bruker) superconducting-magnet NMR spectrometer with TMS as an internal standard. Matrix-assisted laser desorption/ionization time-of-flight (MALDI-TOF) mass spectra were measured on a Shimadzu Kratos Compact MALDI 2 using shinapinic acid as a matrix. UV-vis absorption spectrum was determined on a Shimadzu spectrophotometer (UV 2550). Cyclic voltammetry (CV) measurement was performed on a computer-controlled CHI600D electrochemical analyzer with a Pt working electrode, a Pt plate counter electrode, and an SCE reference electrode immersed in 0.1 M Bu_4NClO_4 in dry acetonitrile purged with dried Argon. The scanning rate was 50 mV/s, and all electrochemical potentials were calibrated with the ferrocene/ferrocenium (Fc/Fc+) standard. The photoluminescence (PL) measurements in different solutions were conducted in a Hitachi F-4600 florescence spectrophotometer. Fluorescence quantum yield was measured by relative method using quinine sulfate as the standard (0.546 in 0.5 mol/L H_2SO_4).

Synthetic Procedures

1-benzylidene-2-phenylhydrazine (1)

To a solution of phenylhydrazine (5.30 g, 50 mmol) in refluxing anhydrous ethanol (100 mL) was added a solution of benzaldehyde (5.40 g, 50 mmol) in anhydrous ethanol (50 mL) dropwise over a period of 20 min. The mixture was stirred at this temperature for 0.5 h. The reaction mixture was allowed to cool to room temperature and the resulting precipitate was collected by filtration and washed with ethanol and dried in vacuum to give 1 as a colorless needle crystal (9.15 g, 93 %). m.p. 154–155 °C. ^{1}H-NMR ($CDCl_3$, 400 MHz): δ 7.66 (s, 1H, HC=N), 7.64 (d, J=2.8 Hz, 2H, phenyl), 7.35 (t, J=14.8, 2H, phenyl), 7.26–7.31 (m, 3H, phenyl), 7.11 (d, J=8.4 Hz, 2H, phenyl), 6.86 (t, J=14.4 Hz, 1H, phenyl).

1-(benzylideneamino)indoline-2,3-dione (2) [22]

To a solution of oxalyl chloride (5.04 g, 40 mmol) in refluxing dichloromethane (50 mL) was added dropwise in 2 h with stirring benzaldehyde phenylhydrazone (7.84 g, 40 mmol) dissolved in dichloromethane (50 mL). The solution was stirred and refluxed 2 h. The reaction mixture was cooled in ice-water bath, and $AlCl_3$ (9 g, 67.5 mmol) was added portionwise but rapidly, and the mixture was refluxed overnight. After cooling, the mixture was poured into cold water. The organic layer was washed with dilute HCl, dried over Na_2SO_4, and evaporated to dryness. The product was purified by column chromatography using silica gel and trichloromethane as the eluent to give 2 as a red solid (7.53 g, 75 %). m.p. 143–144 °C. ^{1}H-NMR ($CDCl_3$, 400 MHz): δ 9.69 (s, 1H, HC=N), 7.80 (d, J=7.6 Hz, 2H, indoline ring), 7.59–7.66 (m, 2H, phenyl), 7.43 (d, J=6.8 Hz, 4H, phenyl), 7.15 (t, J=15.2 Hz, 1H, indoline ring).

3-phenylcinnoline-4-carboxylic acid (3) [22]

Compound 2 (5 g, 20 mmol) from the previous experiment was added to an aqueous solution of potassium hydroxide [prepared by dissolving KOH (30 g, 0.536 mol) in water (30 mL)]. The mixture was heated under reflux for 2 h, then

diluted carefully with boiling water and extracted with chloroform. The aqueous solutions were combined and acidified to pH 4 with concentrated HCl. The precipitate was filtered off, washed with water, and recrystallized in ethanol to give a yellow prism (4.32 g, 86 %). m.p. 233–234 °C. ^{1}H-NMR ($CDCl_3$, 400 MHz) δ 14.57 (br, 1H, -COOH), 8.61 (d, *J*=7.6 Hz, 1H, cinnoline ring), 8.01–8.06 (m, 3H, cinnoline ring), 7.84 (d, *J*=8 Hz, 2H, phenyl), 7.56–7.62 (m, 3H, phenyl).

3-phenylcinnoline (pcl) (4)

A mixture of 3 (3 g, 12 mmol), NaCl (5 g, 85.6 mmol), DMSO (50 mL), and H_2O (5 mL) was stirred at 120 °C for 6 h. After cooling, the mixture was poured into cold water and extracted with ethyl acetate. The organic layer was washed with saturated NaCl solution, dried over Na_2SO_4, and evaporated to dryness. The residue was purified by column chromatography on silica gel with trichloromethane as eluent to give 4 as a yellow needle (1.98 g, 80 %). m.p. 112–113 °C. FT-IR (KBr pellet, cm^{-1}): 1,588, 1,439, 1,326, 1,094, 906, 748, 702. ^{1}H-NMR ($CDCl_3$, 400 MHz) δ 8.58 (d, *J*=8.4 Hz, 1H, cinnoline ring), 8.21–8.25 (m, 3H, cinnoline ring), 7.88 (d, *J*=8 Hz, 1H, cinnoline ring), 7.81 (t, *J*=15.2 Hz, 1H, phenyl), 7.74 (t, *J*=14.8 Hz, 1H, phenyl), 7.55 (t, *J*=14.8 Hz, 2H, phenyl), 7.48 (t, *J*=14.4 Hz, 1H, phenyl).

Ir(pcl)$_2$(pic) (pic=picolinic acid)

To a round-bottomed flask (50 mL), compound 4 (0.33 g, 1.6 mmol), $IrCl_3 \cdot 3H_2O$ (0.2 g, 0.63 mmol), 2-ethoxyethanol (15 mL) and H_2O (5 mL) were added sequentially. The mixture was stirred under nitrogen at 120 °C for 24 h and cooled to room temperature. The precipitate was filtered off, washed with ethanol and acetone and dried in vacuum to give 5 as a dark red solid (0.2 g, 53 %). In a round-bottomed flask (50 mL), a mixture of compound 5 (0.1 g, 0.17 mmol), picolinic acid (0.042 g, 0.34 mmol), triethylamine (1 mL) and dichloromethane (30 mL) was stirred at room temperature for 12 h. The solvent was evaporated, and the product was purified by column chromatography (silica gel, eluent dichloromethane/methanol, 20:1, v/v) to give Ir(pcl)$_2$(pic) as a dark red solid (0.057 g, 65 %). FT-IR (KBr pellet, cm^{-1}): 1,628, 1,588, 1,360, 1,332, 1,258, 1,095, 1,038, 798. ^{1}H-NMR ($CDCl_3$, 400 MHz) δ 8.47 (d, *J*=8 Hz, 1H, pic ring), 8.35 (d, *J*=12 Hz, 2H, cinnoline ring), 8.25 (d, *J*=8 Hz, 1H, pic ring), 7.86–7.90 (m, 3H, cinnoline ring and pic ring), 7.80 (t, *J*=16 Hz, 1H, pic ring), 7.71–7.75 (m, 3H, cinnoline ring), 7.66 (d, *J*=4 Hz, 3H, cinnoline ring), 7.60 (d, *J*=8 Hz, 2H, phenyl), 6.96 (t, *J*=16 Hz, 1H, phenyl), 6.87 (t, *J*=12 Hz, 1H, phenyl), 6.76 (t, *J*=16 Hz, 1H, phenyl), 6.69 (t, *J*=12 Hz, 1H, phenyl), 6.24 (d, *J*=8 Hz, 1H, phenyl), 6.11 (d, *J*=8 Hz, 1H, phenyl). MALDI-TOF MS m/z 748.644 ([Ir(pcl)$_2$(pic)+Na]$^+$).

Ir(pcl)$_2$(fpic) (fpic=5-fluoro-2-picolinic acid)

Complex Ir(pcl)$_2$(fpic) was synthesized with the similar method using 5-fluoro-2-picolinic acid in place of picolinic acid as ancillary ligand, the yield of 60 % with brown powder. FT-IR (KBr pellet, cm^{-1}): 1,633, 1,588, 1,332, 1,258, 1,230, 1,100, 1,038, 798. ^{1}H-NMR ($CDCl_3$, 400 MHz) δ 8.46 (d, *J*=8.4 Hz, 1H, fpic ring), 8.36 (d, *J*=15.2 Hz, 2H, cinnoline ring), 8.28 (d, *J*=3.2 Hz, 1H, fpic ring), 7.90 (d, *J*=6.8 Hz, 3H, cinnoline ring and fpic ring), 7.71–7.77 (m, 3H, cinnoline ring), 7.63–7.68 (m, 3H, cinnoline ring), 7.52 (t, *J*=16 Hz, 2H, phenyl), 6.98 (t, *J*=12 Hz, 1H, phenyl), 6.87 (t, *J*=16 Hz, 1H, phenyl), 6.77 (t, *J*=16 Hz, 1H, phenyl), 6.69 (t, *J*=16 Hz, 1H, phenyl), 6.22 (d, *J*=7.6 Hz, 1H, phenyl), 6.08 (d, *J*=7.6 Hz, 1H, phenyl). MALDI-TOF MS m/z 766.639 ([Ir(pcl)$_2$(fpic)+Na]$^+$).

Results and Discussion

Synthesis and Characterization

Scheme 1 represents a general synthetic route to prepare the ligand and the corresponding complexes. The formation of Ir-complexes are reasonably proved by FTIR spectra of Ir(pcl)$_2$(pic) and Ir(pcl)$_2$(fpic), as shown in Fig. S1 in ESI, in which not only the vibration absorptions at 1,588 and 1,094 cm^{-1} attributed to C=N and C=C in cyclometalating ligand are recognized, but also the characteristic absorption peaks at 1,633 and 1,038 cm^{-1} originating from C=N and C=C in ancillary ligand are recognized. The absorptions at 1,718 and 1,263 cm^{-1} in the IR spectra of complexes may be attributed to C=O and C-O stretching vibrations of the carboxyl groups in ancillary ligands. In addition, the broad and strong absorption peak at 3,000~2,500 cm^{-1} associated with O-H stretching vibrations of the carboxyl groups in ancillary ligands is not observed. All of the data suggested that both cyclometalating ligands and ancillary ligands were excellently coordinated with the metal iridium(III).

As shown in Fig. 1, in ^{1}H NMR spectroscopy, the protons such as H1, H2 and H3 which localize in the two same cyclometalating ligands respectively show different chemical shift, and this phenomenon can be understood that the protons have different environment by coordinating with the iridium(III) ion. On the other hand, the protons of pcl in iridium(III) complexes show an upfield shift compared with the same ones in free ligands. For example, this phenomenon is observed for the proton 9 as well as the proton 1 adjacent to the metalated carbon of the cyclometalating ligand. This can be rationalized in terms of the reduction in electron density in the aromatic ring that accompanies cyclometalation. Additionally, the

Scheme 1 Synthesis routes for $Ir(pcl)_2(pic)$ and $Ir(pcl)_2(fpic)$

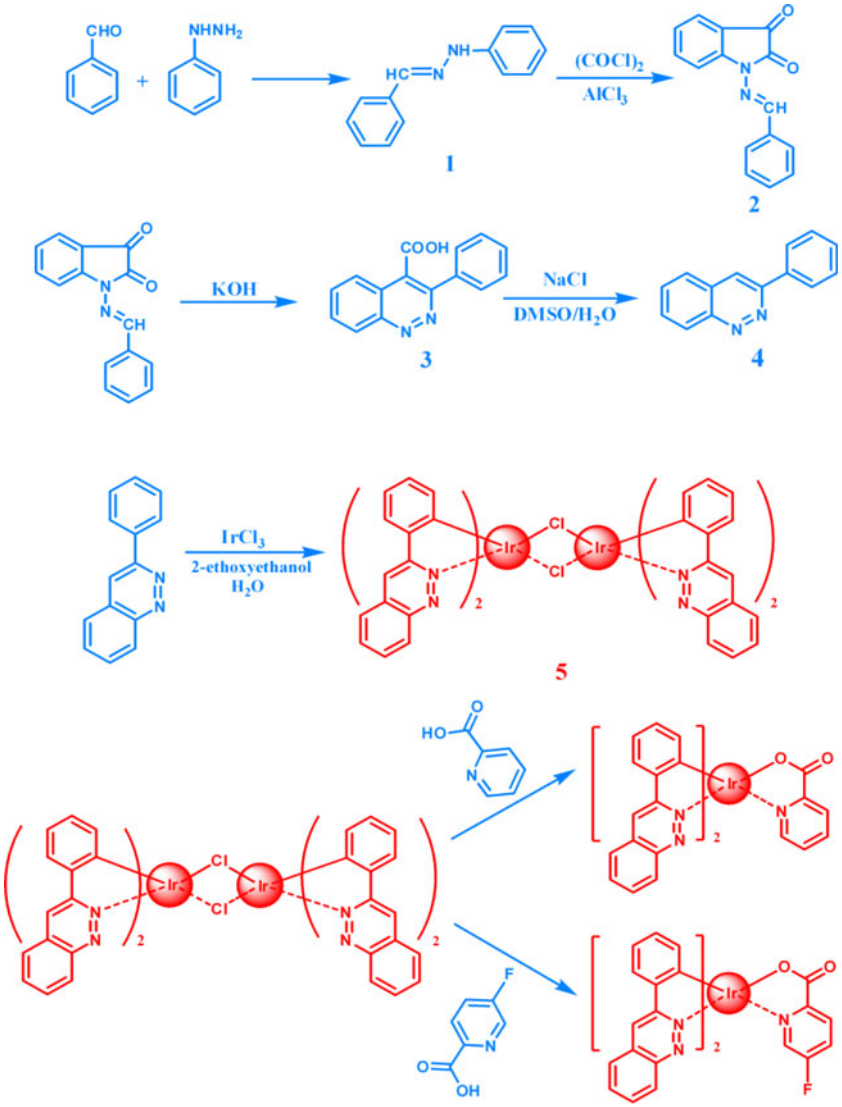

proton of carboxyl group in ancillary ligand disappears, suggesting that the oxygen atom coordinates with iridium(III) ion.

The formation of complexes was further supported by MALDI-TOF mass spectrometry (as seen in Fig. S2). The most abundant peak was 748.644 m/z, which corresponded to the molecular mass of $[Ir(pcl)_2(pic)+Na]^+$. The most abundant signal in mass spectroscopy of $Ir(pcl)_2(fpic)$ was obtained at 766.639 m/z, and the corresponding molecule might be formulated as $[Ir(pcl)_2(fpic)+Na]^+$. We tried to obtain single crystals of these complexes, but failed. Thus, the optimized molecular structures of $Ir(pcl)_2(pic)$ and $Ir(pcl)_2(fpic)$ predicted by the Sparkle/PM6 model are displayed in Fig. 2. The polyhedrons in two complexes are both formed by two carbon atoms and two nitrogen atoms of cyclometalating ligands, one nitrogen atom and one oxygen atom of ancillary ligand. The Ir(III) ion localizes in the center of a distorted octahedral environment, which is consistent with literature reports [23, 24].

UV-vis Absorption of $Ir(pcl)_2(pic)$ and $Ir(pcl)_2(fpic)$

Figure 3 shows the UV-vis absorption spectra of cyclometalating ligand, ancillary ligands and iridium(III) complexes in $CHCl_3$. Because of the similar characteristics of ancillary ligands, the absorption spectra of the two complexes are almost the same. The absorption bands at around 260–350 nm in the ultraviolet region are thought to be due to the ligand-centered LC ($\pi-\pi^*$) transitions, which is located in the same region of absorption spectrum for pcl. The absorption intensities of $Ir(pcl)_2(pic)$ and $Ir(pcl)_2(fpic)$ in this area are weaker than that of free ligands. Moreover, the maximum absorptions of ancillary ligands at around 260 nm also disappear in the spectra of $Ir(pcl)_2(pic)$ and $Ir(pcl)_2(fpic)$. These observations imply the presence of specific electron transfer processes in these iridium(III) complexes. On the other hand, according to the photophysical studies on related iridium(III) complexes, the most intense absorption bands at around 360–410 nm

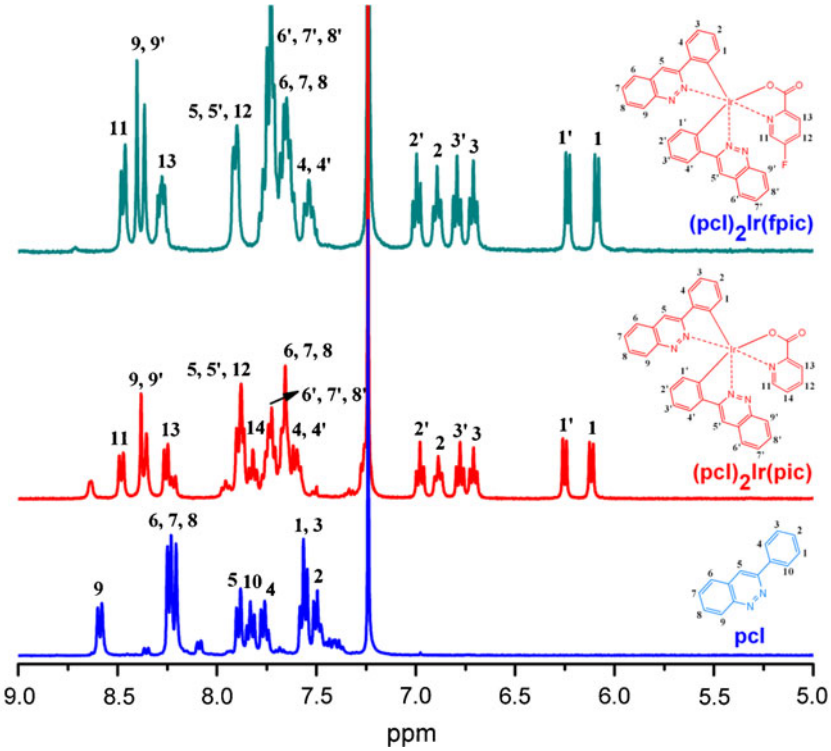

Fig. 1 ^{1}H NMR spectra of pcl, $Ir(pcl)_2(pic)$ and $Ir(pcl)_2(fpic)$ at 400 MHz in $CDCl_3$

and the relatively weak absorption at 470–500 nm can be respectively assigned to the spin-allowed singlet metal-to-ligand charge-transfer (^{1}MLCT) and the spin-forbidden triplet metal-to-ligand charge-transfer (^{3}MLCT) transitions, which are not seen in the absorption spectra of free ligands. The absorption like long tail with higher wavelength and lower energy at around 470–500 nm is gained by mixing of the ^{3}MLCT level with the ^{1}MLCT due to the strong spin-orbit coupling caused by the iridium(III) center. The results also suggest that strong spin-orbit coupling are present to effectively mix the singlet and triplet excited states.

Excitation and Emission Spectra of $Ir(pcl)_2(pic)$ and $Ir(pcl)_2(fpic)$

Figure 4 gives the excitation spectra of $Ir(pcl)_2(pic)$ and $Ir(pcl)_2(fpic)$ with a concentration of 1×10^{-5} mol/L in $CHCl_3$ solution. These spectra show the most intense emission peaks under different excitation wavelengths. In all measurement range, the excitation bands for $Ir(pcl)_2(fpic)$ are relatively more intense than that of $Ir(pcl)_2(pic)$. The reason will be discussed later. The excitation with maximum efficiency at about 366 nm

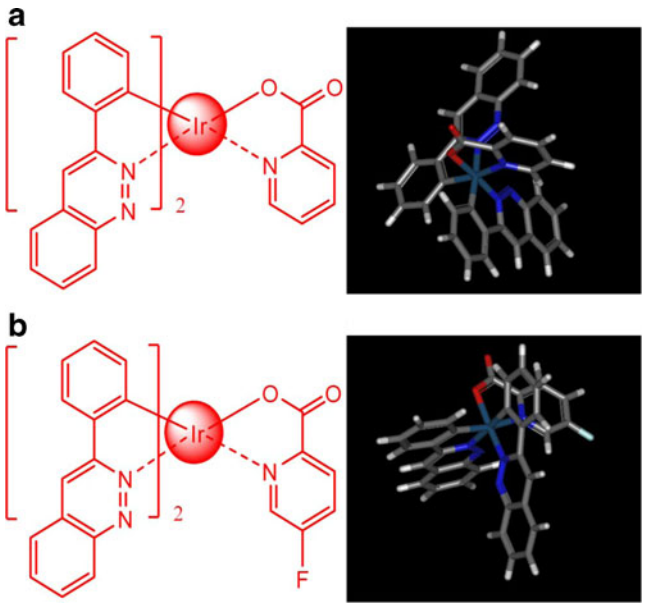

Fig. 2 The ground state geometry of $Ir(pcl)_2(pic)$ (**a**) and $Ir(pcl)_2(fpic)$ (**b**) calculated using the Sparkle/PM6 model

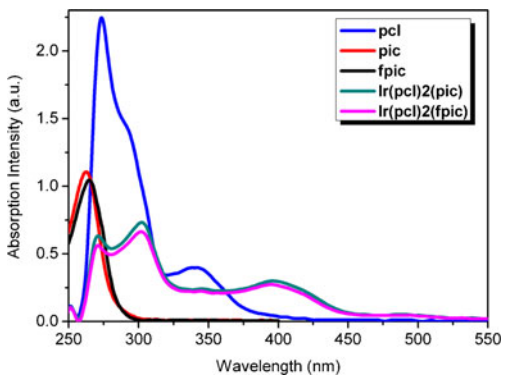

Fig. 3 UV-vis spectra of pcl, $Ir(pcl)_2(pic)$ and $Ir(pcl)_2(fpic)$ in $CHCl_3$ solution with a concentration of 1×10^{-5} mol/L

is correlated to LC ($\pi-\pi^*$) absorption of ligands. The excitation bands at 424 nm and 467 nm are likely to be assigned to ^{1}MLCT and ^{3}MLCT absorptions. Compared with the absorption spectra of two complexes, the excitation bands of Ir(pcl)$_2$(pic) and Ir(pcl)$_2$(fpic) give a good match to their absorption spectra. Moreover, no excitation band is observed in the region of emission, suggesting that the efficient energy transfer can be obtained in two complexes.

Room-temperature photoluminescence (PL) spectra of two complexes are shown in Fig. 5. Luminescence measurements are conducted on $CHCl_3$ solution using 370 nm excitation of the longest wavelength absorption in each case. Deep red emission is observed for Ir(pcl)$_2$(pic), of which PL maxima (λ_{PL}) is observed at 647 nm. The full width at half maximum (FWHM) of this transition is 93 nm. It should be noticed that introducing one fluoro group in the ancillary ligand yields a hypsochromic shift of 6 nm in the PL spectrum of Ir(pcl)$_2$(fpic) (λ_{PL}=641 nm), accompanied by FWHM of 90 nm. The PL spectrum of Ir(pcl)$_2$(fpic) shows a significant blue-shifted phosphorescence emission, due to the substitution of fluoro group in the pyridyl ring which increases the HOMO-LUMO gap to achieve the hypsochromic shift in emission color. The most probable reason for this phenomenon is interpreted as follows. The highly effective inter-system crossing to ^{3}MLCT facilitated by the strong spin-orbit coupling occurs after the ^{1}MLCT excitation from iridium to pcl. Considering the triplet energy level of the ancillary ligand (^{3}LX) compared to that of ^{3}MLCT, there are different ways to deactivate for pcl-centered ^{3}MLCT state. Because the level of ^{3}LX locates higher than that of ^{3}MLCT, the emission of Ir(pcl)$_2$(fpic) is attributed to the phosphorescent decay from the ^{3}MLCT state of pcl. For Ir(pcl)$_2$(pic), the decay from the ^{3}LX state of the ancillary ligand, which is resulted from inter-ligand energy transfer (ILET) from ^{3}MLCT state to ^{3}LX state, occurs because the level of ^{3}LX is lower than that of ^{3}MLCT [17]. As shown in Fig. S3 in ESI, the Commission Internationale de L'Eclairage (CIE) coordinates of Ir(pcl)$_2$(pic) and Ir(pcl)$_2$(fpic) are measured to be x=0.675, y=0.325 and x=0.671, y=0.329, which are very close to pure red emission (x=0.67, y=0.33). All these data confirm that Ir(pcl)$_2$(pic) and Ir(pcl)$_2$(fpic) are promising candidates for red phosphorescent materials.

The solution quantum yield of phenylcinnoline iridium complexes were measured using quinine sulfate (0.546 in 0.5 mol/L H_2SO_4) as a standard [25]. The quantum yield is calculated according to the following expression:

$$\Phi = \Phi_r \frac{A_r}{A}\frac{F}{F_r}\frac{n^2}{n_r^2}$$

where the subscript r refer to the reference substance, Φ is the fluorescent quantum yield, A is the absorbance of the solution at the exciting wavelength, F represents the area of the emission fluorescence spectrum, and n is the refractive index of the solvent.

The PL quantum yield of Ir(pcl)$_2$(pic) and Ir(pcl)$_2$(fpic) in $CHCl_3$ solution is ca. 0.80 % and 0.84 %, respectively. This is presumably due to the less vibration of the C-F bond, compared to C-H bond, thus suppressing the nonradiative deactivation of the excited states in solutions [26].

Effect of Solvent on Photophysical Properties for Ir(pcl)$_2$(pic) and Ir(pcl)$_2$(fpic)

The photoluminescence spectra of Ir(pcl)$_2$(pic) and Ir(pcl)$_2$(fpic) in different solvents are investigated when excited with different wavelengths (350–390 nm) and the results indicate that the optimal excitation wavelength is 370 nm, as shown in Figs. 6 and 7. The UV-vis absorption spectra (Fig. 8) and photoluminescence spectra (excited with 370 nm) (Fig. 9) of Ir(pcl)$_2$(pic) and Ir(pcl)$_2$(fpic) in different solvents are tested at room temperature. Similar solvatochromic effects have been observed in related complexes, due to the relative stability of the ground and excited state dipoles [27]. The absorption peaks of the complexes in different solvents are almost the same. This suggests that the polarity of the solvent has very little influence

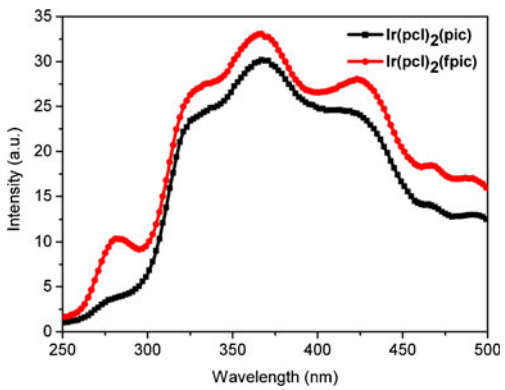

Fig. 4 The excitation spectra of Ir(pcl)$_2$(pic) and Ir(pcl)$_2$(fpic) in $CHCl_3$ solution (1×10^{-5} mol/L)

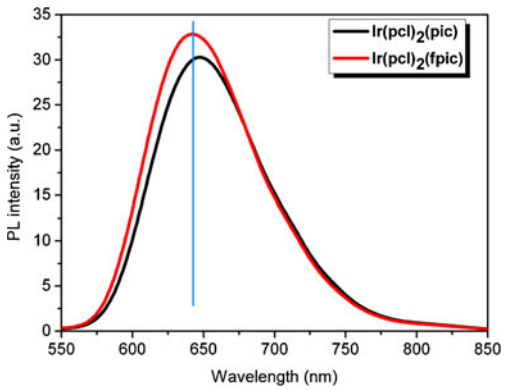

Fig. 5 The emission spectra of Ir(pcl)$_2$(pic) and Ir(pcl)$_2$(fpic) in $CHCl_3$ solution (1×10^{-5} mol/L) (λ_{ex}=370 nm)

on the energy levels of complexes ground state molecules. In this case, however, the emission peaks of $Ir(pcl)_2(pic)$ and $Ir(pcl)_2(fpic)$ in different solvents show clear differences. It may be found that with the polarity of the solvent increasing (Dimethyl sulfoxide > Dimethylformamide > Acetone > Tetrahydrofuran > Trichloromethane), the emission maximum wavelengths are obviously red-shifted from 647 nm in trichloromethane to 671 nm in dimethyl sulfoxide. The peak shift can be attributed to the stronger interaction between the solvents and the excited molecules. Solvents with high polarity can stabilize the excited state of complexes and thus decrease energy content [28]. In addition, compared to other solvents, the PL intensity for both $Ir(pcl)_2(pic)$ and $Ir(pcl)_2(fpic)$ is superimposable in trichloromethane. The differences can be

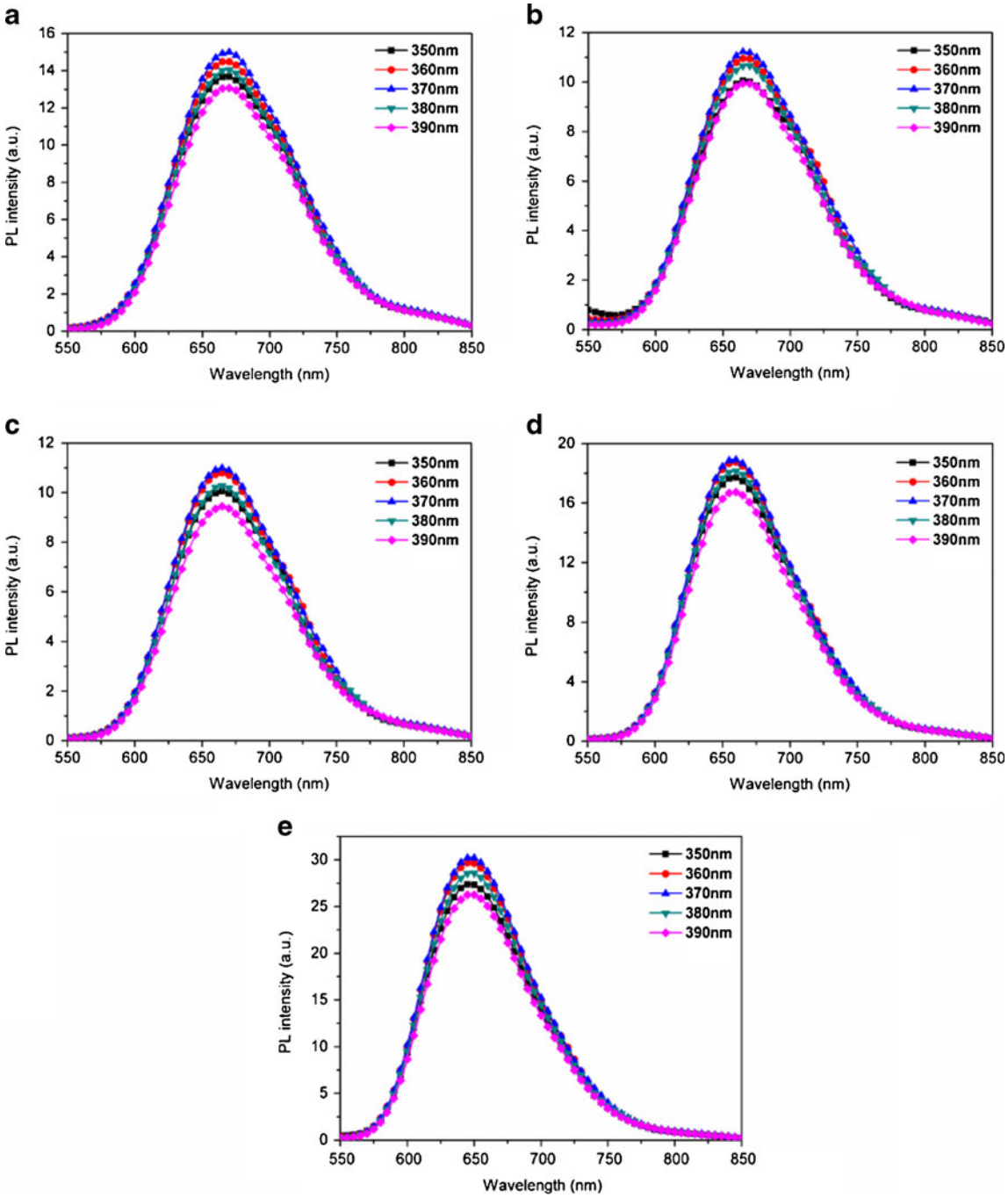

Fig. 6 PL emission spectra of $Ir(pcl)_2(pic)$ under different excitation wavelengths (1×10^{-5} mol/L) (**a** Dimethyl sulfoxide, **b** Dimethylformamide, **c** Acetone, **d** Tetrahydrofuran, **e** Trichloromethane)

clarified by comparing the polarizability of solvent, which is described as the following equation:

$$\Delta f = \left(\frac{\varepsilon-1}{2\varepsilon+1} - \frac{n^2-1}{2n^2+1}\right)$$

In the above expression, ε is the dielectric constant of solvent, n is the refractive index of the solvent, and Δf is the polarizability of solvent. The polarizability and related parameters of different solvents are summarized in Table S1 in ESI. F^a and F^b is the area of the emission fluorescence spectra of $Ir(pcl)_2(pic)$ and $Ir(pcl)_2(fpic)$ respectively, which represent the emission intensities of these complexes. The results show that with the polarizability of solvent increasing, the photoluminescence intensities of two complexes obviously decrease. Generally, the main decay routes of

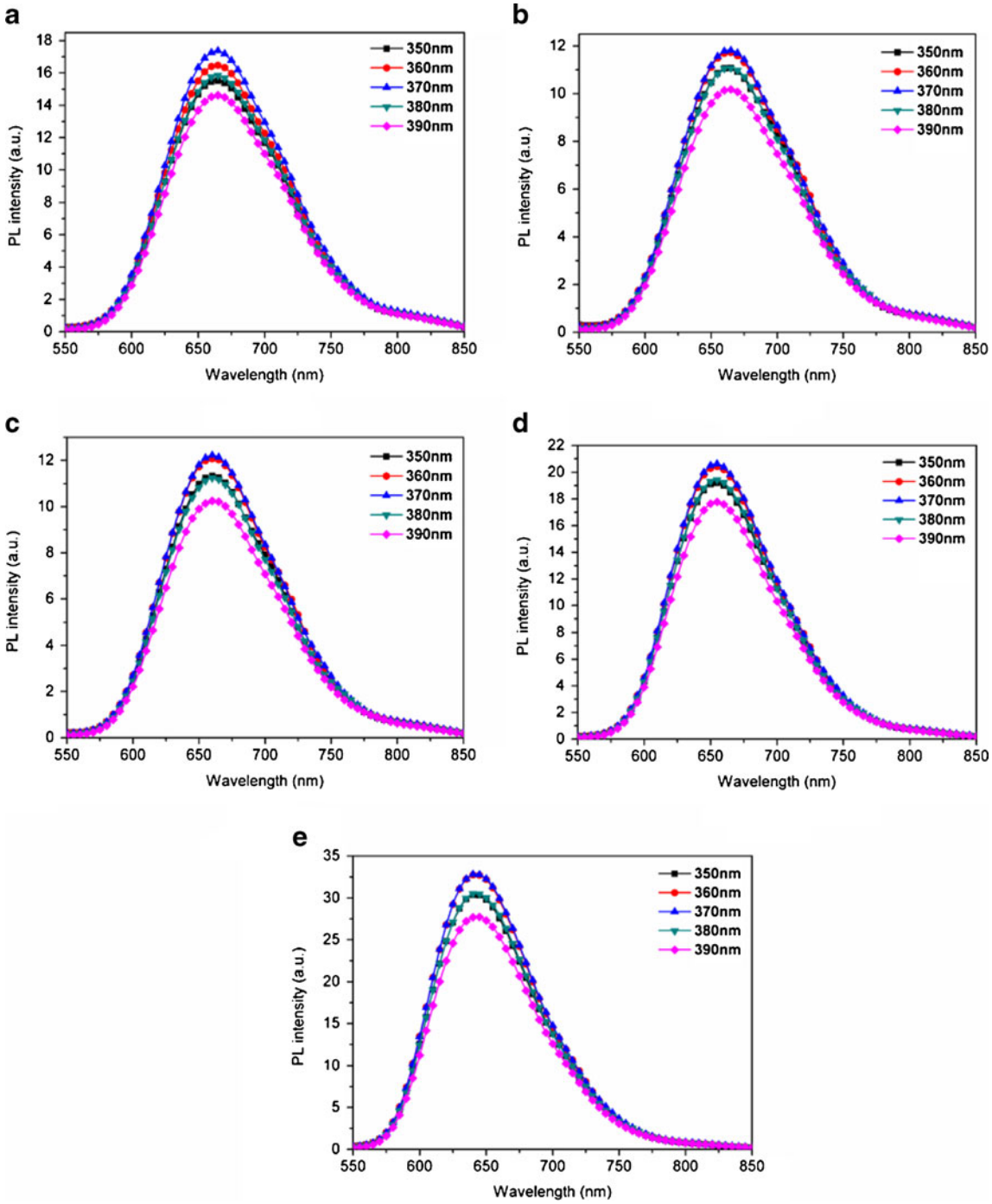

Fig. 7 PL emission spectra of $Ir(pcl)_2(fpic)$ under different excitation wavelengths (1×10^{-5} mol/L) (**a** Dimethyl sulfoxide, **b** Dimethylformamide, **c** Acetone, **d** Tetrahydrofuran, **e** Trichloromethane)

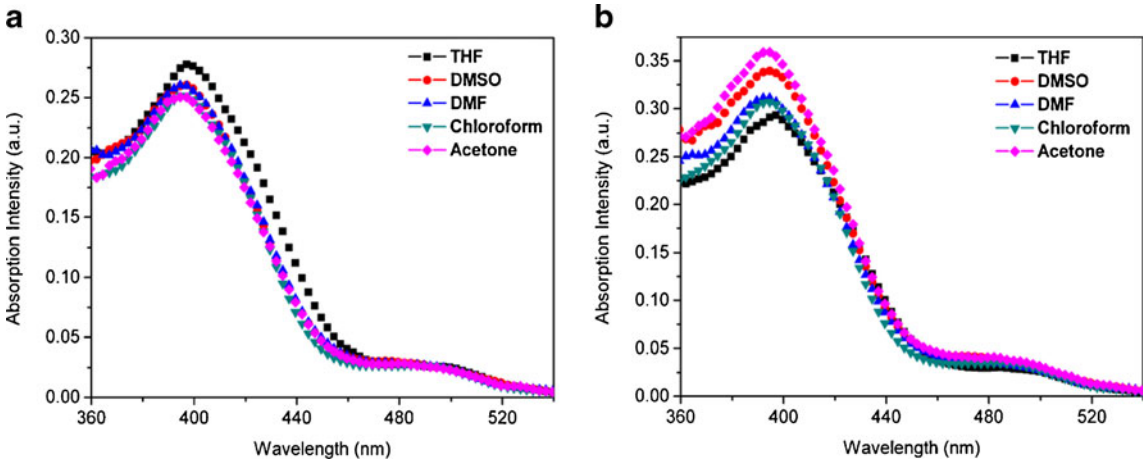

Fig. 8 UV-vis spectra of $Ir(pcl)_2(pic)$ (**a**) and $Ir(pcl)_2(fpic)$ (**b**) in different solvents (1×10^{-5} mol/L)

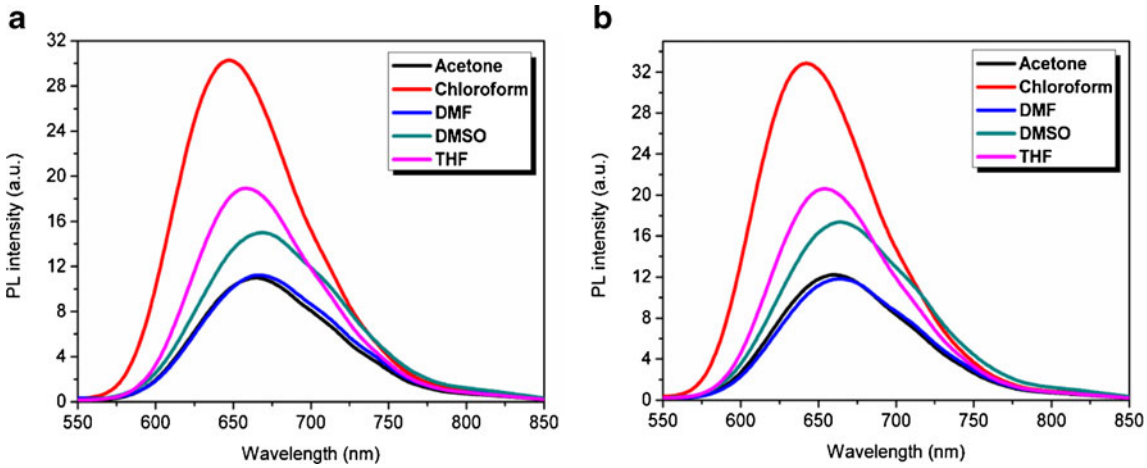

Fig. 9 The emission spectra of $Ir(pcl)_2(pic)$ (**a**) and $Ir(pcl)_2(fpic)$ (**b**) in different solvents (1×10^{-5} mol/L)

the excited state of iridium(III) complexes include radiative and non-radiative. In addition, the polarizability of solvent reflects the deformability of molecules in impressed field, and the value of Δf is higher, the larger deformation of molecules will be obtained. After the formation of excited states, the strong interaction between the solvents and the iridium(III) complexes molecules occurs, and this force leads to the deformation of solvents molecules which is instability. Consequently, the energy of non-radiative increases because that the solvent molecules have a trend to be deformed. It is presumably that the non-radiative deactivation of the excited states of iridium complexes can be brought down in the solvent with small deformation.

Thermal Properties of $Ir(pcl)_2(pic)$ and $Ir(pcl)_2(fpic)$

The thermal properties of the complexes are characterized by thermal gravimetric analysis (TGA). As seen in Fig. S4 in ESI, all the complexes have good stability, and the 5 % weight loss temperatures are 170 °C for $Ir(pcl)_2(pic)$ and 196 °C for $Ir(pcl)_2(fpic)$. The residue of $Ir(pcl)_2(pic)$ and $Ir(pcl)_2(fpic)$ is 17.2 % and 53.6 % at 800 °C, respectively. The thermal analysis demonstrate that $Ir(pcl)_2(fpic)$ is more stable than its analogue, $Ir(pcl)_2(pic)$, suggesting that the introduction of fluoro group into ancillary ligand slightly improves the pyrolysis temperature of the complexes. The formation of intermolecular hydrogen bonds with the

Table 1 Electrochemical data and energy levels of $Ir(pcl)_2(pic)$ and $Ir(pcl)_2(fpic)$

Complex	E_{red} (V)	E_{ox} (V)	HOMO (eV)	LUMO (eV)	E_{gap} (eV)
$Ir(pcl)_2(pic)$	−1.43	1.27	−5.65	−2.95	2.70
$Ir(pcl)_2(fpic)$	−1.44	1.27	−5.65	−2.94	2.71

fluorine atom may be attributed to increase the decomposition temperature [29]. All the above data suggest that complexes $Ir(pcl)_2(pic)$ and $Ir(pcl)_2(fpic)$ are thermally stable enough to experience device construction through vacuum deposition.

Electrochemical Properties of $Ir(pcl)_2(pic)$ and $Ir(pcl)_2(fpic)$

The electrochemical properties of $Ir(pcl)_2(pic)$ and $Ir(pcl)_2(fpic)$ are investigated by cyclic voltammetry (CV) (as shown in Fig. S5 in ESI) using an degassed acetonitrile solution in presence of 0.1 M Bu_4NClO_4 as a supporting electrolyte. A Hg/Hg_2Cl_2 electrode is used as a reference electrode; a platinum electrode is used as a working electrode; a platinum plate is used as a counter electrode.

In order to evaluate charge injection and device performance, HOMO-LUMO energy levels of complexes are calculated using cyclic voltammetry [30, 31]. The onset reduction potential ($E_{onset,\ red}$) of $Ir(pcl)_2(pic)$ is estimated to be −1.43 V, while $E_{onset,\ red}$ of $Ir(pcl)_2(fpic)$ is −1.44 V. E_{LUMO} is calculated according to the empirical relationship: $E_{LUMO}=-(E_{onset,\ red}+4.38)$ (eV). The energy band gap between HOMO and LUMO energy levels is determined from the optical absorption spectrum ($E_g=1{,}240/\lambda_{a,\ edge}$) and a HOMO energy level is obtained from the equation: E_{HOMO} (eV)=E_{LUMO} - Eg. The summarized E_{red}, E_{ox}, HOMO, LUMO, and E_{gap} data of the iridium complexes are shown in Table 1. Though these close oxidation potentials obtained under identical conditions indicate that the substitution of fluoro group in the pyridyl ring does not affect the oxidative process of the iridium complexes very much, the energy gap of $Ir(pcl)_2(fpic)$ is little higher than that of $Ir(pcl)_2(pic)$, which is consistent with the emission spectra of $Ir(pcl)_2(pic)$ and $Ir(pcl)_2(fpic)$. Substituent effect of iridium can be transmitted through carbon atom-iridium bonding, and the energy gap is also controlled by the characteristic of cyclometalating ligands or ancillary ligands. The electrochemical studies of these complexes demonstrate that the electron withdrawing fluorine group in ancillary ligands increases the energy gap between the HOMO level and the LUMO level.

Conclusions

Two novel complexes $Ir(pcl)_2(pic)$ and $Ir(pcl)_2(fpic)$ have been successfully synthesized with 3-phenylcinnoline, and picolinic acid and 5-fluoro-2-picolinic acid were chosen as ancillary ligands to investigate the effect of substitution in pyridyl ring. The formations of $Ir(pcl)_2(pic)$ and $Ir(pcl)_2(fpic)$ were confirmed by FTIR, ^1H NMR and MALDI-TOF mass spectrometry. The thermal properties of these complexes were measured and high thermal stability was demonstrated. The photoluminescence spectra of $Ir(pcl)_2(pic)$ and $Ir(pcl)_2(fpic)$ have been studied and the results showed that two complexes all exhibited saturated red emission. Especially, the effects of excitation wavelength and solvents on emission spectra were detailed discussed, the results showed that the optimal excitation wavelength was 370 nm, and the polarity of solvent had important influence for emission spectrum.

Acknowledgments The authors appreciate the Guangdong-Hongkong Technology Cooperation Finding (Project No. 2009A091300012).

References

1. Pei Q, Yu G, Zhang C, Yang Y, Heeger AJ (1995) Polymer light-emitting electrochemical cells. Science 269:1086–1088
2. Tordera D, Delgado M, Orti E, Bolink HJ, Frey J, Nazeeruddin MK, Baranoff E (2012) Stable green electroluminescence from an iridium tris-heteroleptic ionic complex. Chem Mater 24:1896–1903
3. Wu HB, Chen HF, Liao CT, Su HC, Wong KT (2012) Efficient and color-stable solid-state white light-emitting electrochemical cells employing red color conversion layers. Org Electron 13:483–490
4. Marin-Suarez M, Curchod BFE, Tavernelli I, Rothlisberger U, Scopelliti R, Jung I, Di Censo D, Gratzel M, Fernandez-Sanchez JF, Fernandez-Gutierrez A, Nazeeruddin MK, Baranoff E (2012) Nanocomposites containing neutral blue emitting cyclometalated iridium(III) emitters for oxygen sensing. Chem Mater 24:2330–2338
5. Mark CSK, Pentlehner D, Stich M, Wolfbeis OS, Chan WK, Yersin H (2009) Exceptional oxygen sensing capabilities and triplet state properties of Ir(ppy-NPh2)(3). Chem Mater 21:2173–2175
6. Ho ML, Chen YA, Chen TC, Chang PJ, Yu YP, Cheng KY, Cheng CH, Shih CH, Lee GH, Sheu HS (2012) Synthesis, structure and oxygen-sensing properties of Iridium(III)-containing coordination polymers with different cations. Dalton Trans 41:2592–2600
7. DeRosa MC, Hodgson DJ, Enright GD, Dawson B, Evans CEB, Crutchley RJ (2004) Iridium luminophore complexes for unimolecular oxygen sensors. J Am Chem Soc 126:7619
8. Zhou M, Fei H, Liu Y, Li WF (2010) Metal complexes and their applications in bioassay, bio-imaging and protein staining. Prog Chem 22:201–209
9. Lowry MS, Bernhard S (2006) Synthetically tailored excited states: phosphorescent, cyclometalated iridium(III) complexes and their applications. Chem Eur J 12:7970–7977
10. Lo KKW, Chung CK, Zhu N (2003) Synthesis, photophysical and electrochemical properties, and biological labeling studies of cyclometalated iridium(III) Bis(pyridylbenzaldehyde) complexes: novel luminescent cross-linkers for biomolecules. Chem Eur J 9:475–483
11. Xiao LX, Chen ZJ, Qu B, Luo JX, Kong S, Gong QH, Kido JJ (2011) Recent progresses on materials for electrophosphorescent organic light-emitting devices. Adv Mater 23:926–952
12. Bolink HJ, Angelis FD, Baranoff E, Klein C, Fantacci S, Coronado E, Sessolo M, Kalyanasundaram K, Grätzel M, Nazeeruddin MK (2009) White light phosphorescence emission from a single molecule: application to OLED. Chem Commun 4672–4674
13. Chen ZQ, Bian ZQ, Huang CH (2010) Functional Ir(III) complexes and their applications. Adv Mater 22:1534–1539
14. Jayaraman J, Venugopal T, Kanagarathinam S, Natesan S (2011) Iridium(III) complexes with orthometalated phenylimidazole ligands subtle turning of emission to the saturated green colour. J Fluoresc 21:507–519
15. Flamigni L, Barbieri A, Sabatini C, Ventura B, Barigelletti F (2007) Photochemistry and photophysics of coordination compounds: iridium. Top Curr Chem 281:143–203

16. Lamansky S, Djurovich P, Murphy D, Abdel-Razzaq F, Lee HE, Adachi C, Burrows PE, Forrest SR, Thompson ME (2001) Highly phosphorescent Bis-cyclometalated iridium complexes: synthesis, photophysical characterization, and use in organic light emitting diodes. J Am Chem Soc 123:4304–4312
17. You Y, Park SY (2005) Inter-ligand energy transfer and related emission change in the cyclometalated heteroleptic iridium complex: facile and efficient color tuning over the whole visible range by the ancillary ligand structure. J Am Chem Soc 127:12438–12439
18. Hao YY, Guo XX, Lei LP, Yu JN, Xu HX, Xu BS (2010) Multicolor emitting from a single component emitter: new iridium(III) complexes with ancillary ligand 2-(2-hydroxyphenyl) benzothiazole. Synth Met 160:1210–1215
19. Tong B, Mei Q, Wang S, Fang Y, Meng Y, Wang B (2008) Nearly 100 % internal phosphorescence efficiency in a polymer light-emitting diode using a new iridium complex phosphor. J Mater Chem 18:1636–1639
20. Fang Y, Tong B, Hu S, Wang S, Meng Y, Peng J, Wang B (2009) A highly efficient tris-cyclometalated iridium complex based on phenylphthalazine derivative for organic light-emitting diodes. Org Electron 10:618–622
21. Mi B, Wang P, Gao Z, Lee C, Lee S, Hong H, Chen X, Wong M, Xia P, Cheah K, Chen C, Huang W (2009) Strong luminescent iridium complexes with C^N=N structure in ligands and their potential in efficient and thermally stable phosphorescent OLEDs. Adv Mater 21:339–343
22. Lowrie HS (1966) 3-Phenylcinnolines. I. Some reactions and derivatives of 3-phenylcinnoline −4-carboxylic acids. J Med Chem 9:664–669
23. Laskar IR, Chen TM (2004) Tuning of wavelengths: synthesis and photophysical studies of iridium complexes and their applications in organic light emitting devices. Chem Mater 16:111–117
24. Chin CS, Eum MS, Kim SY, Kim C, Kang SK (2007) Blue-light-emitting complexes: cationic (2-phenylpyridinato)iridium(III) complexes with strong-field ancillary ligands. Eur J Inorg Chem 3:372–375
25. Crosby GA, Demas JN (1971) Measurement of photoluminescence quantum yields. Review. J Phys Chem 75:991–1024
26. Ivanov P, Stanimirov S, Kaloyanova S, Petkov I (2012) Synthesis and photophysical properties of yellow-emitting iridium complexes. Effect of the temperature on the character of triplet emission. J Fluoresc 22:1501–1507
27. Goldstein DC, Cheng YY, Schmidt TW, Bhadbhade M, Thordarson P (2011) Photophysical properties of a new series of water soluble iridium bisterpyridine complexes functionalized at the 4′ position. Dalton Trans 40:2053–2061
28. Zhang YQ, Song MJ, Huang LQ (2012) A novel blue-emitting Ir(III) complex with short excited state lifetime: synthesis, structure, photophysical property, and electrophosphorescence performance. J Lumin 132:2242–2246
29. Zhang WG, Wang YS, He ZQ, Mu LP, Zou Y, Liang CJ, Zhao SM (2010) Efficient electrophosphorescence based on 2-(9,9-diethylfluoren-2-yl)-5- trifluoromethylpyridine iridium complexes. Synth Met 160:354–360
30. Sun JY, He ZQ, Mu LP, Han X, Wang JL, Wang B, Liang C, Wang YS, Liu Y, Cao S (2007) Preliminary photovoltaic response from a polymer containing *p*-vinylenephenylene amine backbone. Solar energy mater. Solar Cells 91:1289–1298
31. Zhang WG, He ZQ, Hui GB, Mu LP, Wang YS, Zhao SM, Jing XP (2009) Synthesis and light-emitting properties of 2-(N-phenyl-alpha-naphthylamino) and 2-dimesitylboron-7-(N -phenyl-alpha-naphthylamino)-9,9-diethylfluorene. Sci Chin Ser B Chem 52:952–960